2012

Two-Photon Cooperative Absorption in Colliding Cold Na Atoms

PHYSICAL REVIEW LETTERS, COLLEGE PK, v. 108, n. 25, supl. 1, Part 1, pp. 232-238, 43617, 2012

Two-Photon Cooperative Absorption in Colliding Cold Na Atoms

E. Pedrozo-Peñafiel, R. R. Paiva, F. J. Vivanco, V. S. Bagnato, and K. M. Farias
Instituto de Física de São Carlos, Universidade de São Paulo, São Paulo, Brasil
(Received 28 December 2011; published 19 June 2012)

Two-photon cooperative absorption is common in solid-state physics. In a sample of trapped cold atoms, this effect may open up new possibilities for the study of nonlinear effects. The experiment described herein starts with two colliding Na atoms in the S hyperfine ground state. The pair absorb two photons, resulting in both a $P_{1/2}$ and a $P_{3/2}$ atom. This excitation is observed by ionization using an external light source. A simple model that considers only dipole-dipole interactions between the atoms allows us to understand the basic features observed in the experimental results. Both the pair of generated atoms and the photons originating from their decay are correlated and may have interesting applications that remain to be explored.

DOI: 10.1103/PhysRevLett.108.253004 PACS numbers: 32.80.−t, 34.50.Cx, 67.85.−d

In many atomic processes, it is common for a pair of atoms or molecules to absorb a single photon. In fact, such processes were fundamental to the development of the understanding of cold collisions [1] and the determination of scattering length values [1], among others. It is possible, however, that two atoms can be simultaneously excited by a coherent two-photon absorption. This effect was first observed in a mixture of Ba/Tl, where a pair of atoms were simultaneously excited by a cooperative-absorption process [2]. The problem has also been considered theoretically by a few authors [3,4].

While colliding cold atoms have been a test bench for many studies [5], nonlinear optical effects involving two-photon absorption have not been deeply investigated in this system. In a sample of cold atoms, the absence of motion and the long-range part of the interaction guarantee the necessary ingredients for a two-photon cooperative absorption, making this sample adequate for studying cooperative transitions near resonances. In this Letter, we demonstrate the *occurrence of a two-photon cooperative absorption* in a pair of colliding cold Na atoms kept in a magneto-optical trap [6]. Two photons from a *strong* laser having a frequency ω are absorbed by a cooperating pair of atoms producing $3P_{1/2}$ and $3P_{3/2}$ excited atoms when the relationship $2\omega = \omega_{S\to P_{1/2}} + \omega_{S\to P_{3/2}}$ between the laser frequency ω and the atomic transition frequencies is satisfied. We start with an overview of this effect followed by a description of the experimental system and the obtained results. Finally, we describe a few possible applications for the observed phenomenon.

Consider two colliding Na atoms. For simplicity, the hyperfine structure will not be included. The relevant levels and transitions of interest are presented in the diagrams in Fig. 1. Single-photon transitions in each individual atom as well as the two-photon transitions considered in this work are represented in the diagrams in Figs. 1(a) and 1(b). Without interaction between the atoms, the transition probability for two-photon absorption by the pair will be the product of the two independent one-photon, one-atom transition probabilities. In this case, the two-photon absorption by the two atoms occurs when the probe laser frequency is resonant with one of the atomic transitions [$3S_{1/2} \to 3P_{1/2}$ ($\hbar\omega_{P_{1/2}}$) or $3S_{1/2} \to 3P_{3/2}$ ($\hbar\omega_{P_{3/2}}$)]. When considering a new situation where the atoms can interact, the picture changes; the two-photon absorption by the pair is now possible when $\omega = \frac{\omega_{P_{1/2}} + \omega_{P_{3/2}}}{2}$ once the pair can distribute the energy absorbed and promote each atom to a different excited state.

The ideas for the theoretical basis are presented in Ref. [3], where an electric-dipole interaction is assumed between the incident light and each atom, whereas the interaction between the atoms is considered to be ruled by the dipole-dipole interaction. If we consider the linewidth of both individual transitions as $\hbar\Gamma$ and the dipole

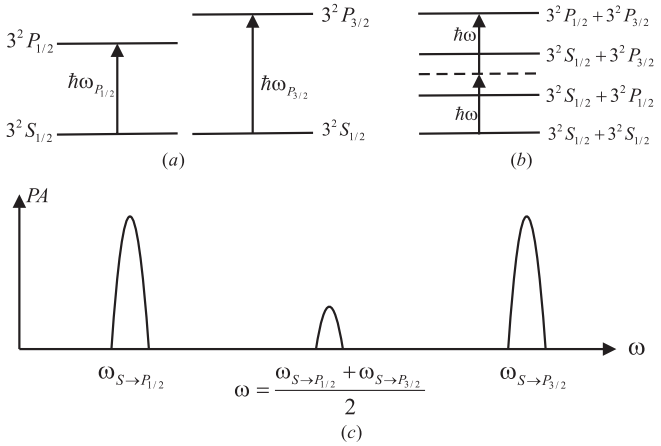

FIG. 1. Diagrammatic representation of the levels and transitions of interest. (a) One-photon transitions in each atom from the ground state to one of the excited states ($3S_{1/2} \to 3P_{1/2}$ and $3S_{1/2} \to 3P_{3/2}$). (b) Two-photon cooperative absorption in both atoms from the ground state to the double excited state ($3S_{1/2} + 3S_{1/2} \to 3P_{1/2} + 3P_{3/2}$). (c) Representation of the probability of absorption (PA) as a function of probe frequency (ω); when ω is equal to $\frac{\omega_{P_{1/2}} + \omega_{P_{3/2}}}{2}$, the presence of atomic interactions makes the transition to the excited states possible.

matrix element of each individual transition as $\mu_{P_{1/2}}$ and $\mu_{P_{3/2}}$, the total probability of absorption (PA) for a system interacting with a laser of frequency ω can be evaluated using second-order perturbation theory in the external field [3]. The final result is that the total absorption probability is

$$PA(\omega) \propto \left[\frac{(\mu_{P_{1/2}} E/2\hbar)^2}{(\omega_{P_{1/2}} - \omega)^2 + (\Gamma/2)^2}\right]\left[\frac{(\mu_{P_{3/2}} E/2\hbar)^2}{(\omega_{P_{3/2}} - \omega)^2 + (\Gamma/2)^2}\right] \times \left[1 + \frac{4\langle H_I\rangle^2/\hbar^2}{(2\omega - \omega_{P_{1/2}} - \omega_{P_{3/2}})^2 + \Gamma^2} + \frac{4(2\omega - \omega_{P_{1/2}} - \omega_{P_{3/2}})\langle H_I\rangle/\hbar}{(2\omega - \omega_{P_{1/2}} - \omega_{P_{3/2}})^2 + \Gamma^2}\right], \quad (1)$$

where E is the electromagnetic field amplitude and $\langle H_I\rangle$ is the matrix element describing the interaction [3].

In the absence of interaction between the atoms ($\langle H_I\rangle = 0$), the probability of absorption peaks when the incident photon is resonant with the atomic transition ($\omega = \omega_{P_{1/2}}$ or $\omega = \omega_{P_{3/2}}$), as indicated by the first two brackets of Eq. (1) and represented by the two major peaks in Fig. 1(c). The last two terms of the third bracket in Eq. (1) show that a new absorption peak, which is the evidence of the two-photon cooperative absorption, appears for $\omega = \frac{\omega_{P_{1/2}} + \omega_{P_{3/2}}}{2}$, i.e., halfway between the two atomic transitions, whereas the unit factor reproduces the result for the case when there is no interaction. If we consider the interaction strength ($\langle H_I\rangle$) to be of the order of magnitude of the linewidth ($\hbar\Gamma$), Ref. [3] indicates that the two-photon contribution is estimated to be three orders of magnitude smaller than the one-photon contribution.

To experimentally demonstrate the two-photon cooperative absorption, we have used a magneto-optical trap containing sodium atoms [7]. An overview of the experimental system is presented in Fig. 2. An oven operating at 550 K generates an effusive atomic beam. The beam is decelerated by a Zeeman slowing technique in a spin-flip configuration [8]. Two dye lasers and a solid-state laser are used to produce all of the frequencies required for the experiment:

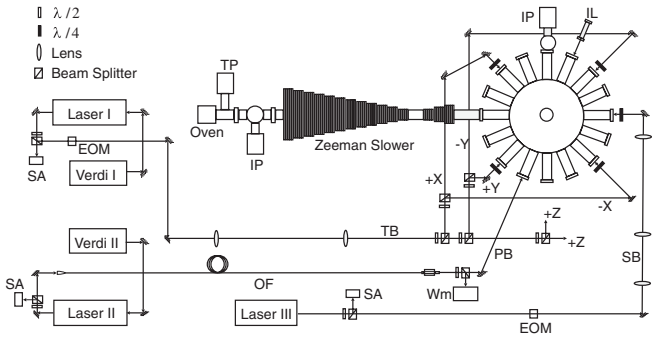

FIG. 2. Schematic representation of the experimental system, where SA denotes saturated absorption; TP, turbo pump; IP, ion pump; Wm, wave meter; IL, ionization laser; EOM, electro-optical modulator; SB, slower beam; PB, probe beam; OF, optical fiber; and TB, trapping beam.

deceleration, trapping, repumper, and probe. The trapping frequency is red-tuned 10 MHz from $3S_{1/2}(F = 2) \rightarrow 3P_{3/2}(F = 3)$ transition [9]. The trapping laser beam passes through an electro-optical modulator, generating a sideband that is resonant with $3S_{1/2}(F = 1) \rightarrow 3P_{3/2}(F = 2)$ transition and that works as a repumper for atoms ending in the wrong hyperfine ground state during the cooling process. The slowing laser is red-tuned 500 MHz from the $3S_{1/2}(F = 2) \rightarrow 3P_{3/2}(F = 3)$ transition. This laser beam also carries a sideband to allow for optical pumping to $3S_{1/2}(F = 2)$ before the atoms enter the slower magnet. The slowing laser is a solid-state commercial laser (TOPTICA TA-SHG pro), whereas the other two are dye lasers (Coherent 899). The probe laser scans through the transitions by intervals of 30 GHz and has its frequency monitored by a wave meter (HighFinesse WS-U).

Once the atoms undergo a transition reaching either of the states $3P_{1/2}$ or $3P_{3/2}$, they are detected using ionization caused by a 405 nm laser. The ionization laser reaches the cloud of cold atoms with an intensity of 11 $\mathrm{mW/cm^2}$ and can ionize any population in the $3P_{1/2}$ level and higher. Once ionized, individual ions are detected by a channeltron particle multiplier located near the trapped cloud [7]. A calibrated photodiode collects the fluorescence from the cold atoms to determine the number of trapped atoms, and a CCD camera is used to obtain the atomic cloud image. Both pieces of information allow the determination of the atomic density. The probe and ionization lasers are overlapped and focused into the atomic cloud following the same pathway. Ions detected by the channeltron are processed by an ion counter [10].

The time sequence for this experiment is shown in Fig. 3. Once the magneto-optical trap is filled with approximately 10^9 atoms, the slowing laser is shut down. At this moment, the probe and ionization lasers are released, and after a Δt, ion counting starts. Alternated time intervals detect the signal [Fig. 3(b)] and background [Fig. 3(a)]. The background is subtracted from the signal. Each frequency point is the result of 300 averages. The whole range of frequencies from $\omega_{P_{1/2}}$ to $\omega_{P_{3/2}}$ is contained in the probe laser scan. After a general scan, we have concentrated around the regions of interest. Detectable ion counts were observed for ω around $\omega_{P_{1/2}}$, $\omega_{P_{3/2}}$ and $\omega = \frac{\omega_{P_{1/2}} + \omega_{P_{3/2}}}{2}$ as presented in Fig. 4 and are in agreement with the prediction of Fig. 1.

The intensity balance between the trap and repumper lasers produces a population of atoms in the $3S_{1/2}(F = 2)$ much larger than the $3S_{1/2}(F = 1)$. We make the approximation that most atomic colliding pairs are in the $3S_{1/2}(F = 2) + 3S_{1/2}(F = 2)$ state. This phenomenon was previously investigated in our experimental system [7].

The final registered signal corresponds to the ions produced by the probe laser only, because we subtract signal A from signal B. During window A of the counter, atoms in the magneto-optical trap are naturally promoted to the $3P_{3/2}$ state by the trapping and repumper beams, and these atoms are ionized and counted. During window B, the

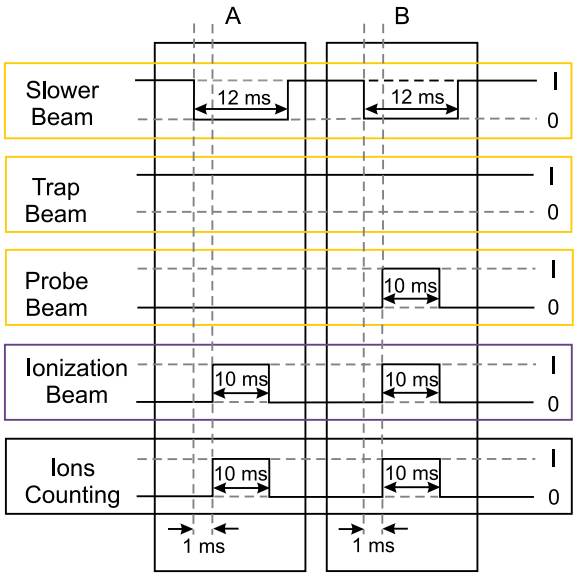

FIG. 3 (color online). The time sequence is divided into two counting windows, A and B. The first counts the ions formed by the ionization of the atoms in the excited states with energies equal to or higher than the $3P_{1/2}$ state due to absorption of the trap frequencies, i.e., the background ion counts. The second window counts the ions formed due to the absorption of the probe laser and the trap frequencies. The trap frequencies remain on during the whole measurement. The ion counts start 1 ms after the slower beam is shut down. The probe frequency is on during the counts in the second measurement window and off in the background counts.

effect of the probe laser is added. In this case, fluctuations can produce negative overall signals.

The peaks related to the one-photon transitions ($\omega = \omega_{P_{1/2}}$ and $\omega = \omega_{P_{3/2}}$) are much larger than the peak related to the two-photon cooperative absorption at $2\omega = \omega_{P_{1/2}} + \omega_{P_{3/2}}$, and they also present shoulders that are related to the hyperfine states of both ground and excited states. While the single-photon excitation peaks reach values up to 6000/s counts of ions, the two-photon excitation stays below 30/s. This large factor is expected based on calculations [3] for a system where $\langle H_I \rangle$ is on the order of $\hbar\Gamma$. Therefore, our interaction strength must be on the order of the line width.

The central peak in Fig. 4 (two-photon cooperative absorption) presents an evident asymmetry, shown in more detail in the small graph in the center. The asymmetry extending to the red part is a consequence of the attractive part of the interatomic potential.

The two single-photon absorption peaks have a verified linear dependence on the probe laser intensity, whereas the central peak amplitude has a quadratic dependence on the probe laser intensity, demonstrating the two-photon process. Figure 5 shows the observed quadratic intensity dependence.

The overall aspect of the data points presented in Fig. 6 extending more to the red part, reaching a maximum and fast decay on the blue side is a consequence of the compromise of two effects, the number of pairs at smaller

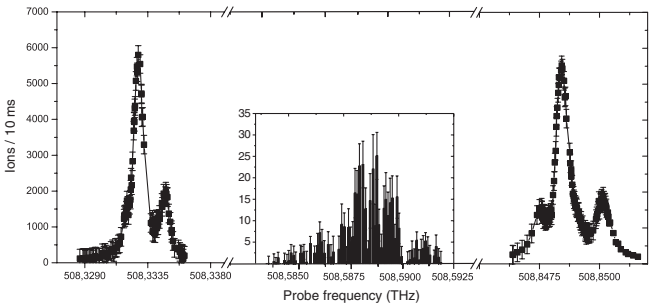

FIG. 4. Ion counts as a function of the probe frequency. From left to right, the first (last) peak is due to the ionization of the atoms excited to the $3P_{1/2}$ ($3P_{3/2}$) state. These peaks have shoulders that are due to hyperfine transitions. The central peak, shown in more detail in the small graph in the center, is evidence of the two-photon cooperative absorption.

internuclear separation and the potential dependence with the atoms' separation. To have a strong two-photon absorption, we need interaction, which can be obtained at the red side of the $\frac{\omega_{P_{1/2}}+\omega_{P_{3/2}}}{2}$ frequency, where the energy levels are curving down due to interaction. In contrast, to the red of resonance, the number of pairs decreases (resonance for pairs at smaller internuclear separation). The combination between those two effects results in the shape observed for the cooperative absorption.

In an attempt to better understand the two-photon cooperative absorption line shape, we have produced a simple model equivalent to the photo-associative ionization calculation presented by Gallagher [11]. The ground-state potential depends on the internuclear separation (R) as R^{-6}, whereas the excited-state potentials go as R^{-3}. Therefore, we can consider the ground-state to be constant at long range and the energy levels of the excited states to have a dependence like $\hbar\omega_j - C_j^{(3)}/R^3$ with $j = 1/2$ or $3/2$. Hence, the energy distance decreases as the atoms approach each other, which shifts the resonance frequency to the red.

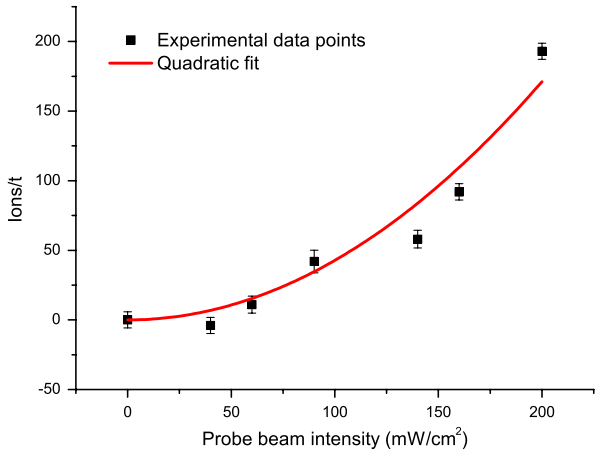

FIG. 5 (color online). Ion counts as a function of the probe intensity. A quadratic fit was plotted to see the expected behavior of two-photon cooperative absorption.

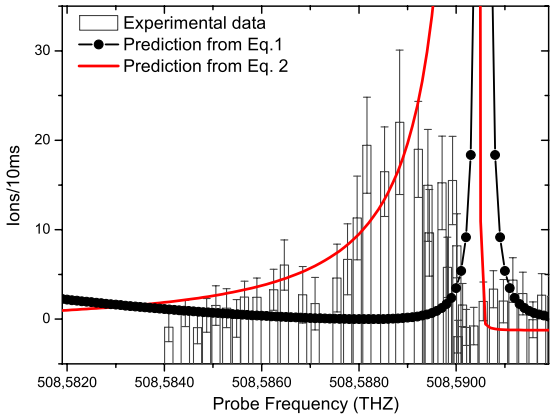

FIG. 6 (color online). Ion counts as a function of the probe laser frequency in the region around the halfway point between the $3P_{1/2}$ and the $3P_{3/2}$ transitions (central peak of Fig. 4). The experimental data are compared with the theoretical curve expected from Eq. (1) (dotted line) and with Eq. (2) (continuous line), which takes into account the R^{-3} dependence of the excited potentials. This finding demonstrates that the peak asymmetry comes from the R^{-3} dependence of the potentials.

Although the number of atoms involved in deeper and deeper collisions goes down for small interatomic distances. We have considered, for the model, that the density of pairs constant as a function of R. Integrating over R [Eq. (2)], we obtain an improvement when compared to Eq. (1). Figure 6 presents, together with experimental data, the models as predicted by Eqs. (1) and (2).

$$PA(\omega) \propto \int_0^\infty dR \Bigg[\frac{(\mu_{P_{1/2}} E/2\hbar)^2}{(\omega_{P_{1/2}} - \frac{C^{(3)}_{1/2}}{R^3} - \omega)^2 + (\Gamma/2)^2} \Bigg] \times \Bigg[\frac{(\mu_{P_{3/2}} E/2\hbar)^2}{(\omega_{P_{3/2}} - \frac{C^{(3)}_{3/2}}{R^3} - \omega)^2 + (\Gamma/2)^2} \Bigg] \times \Bigg[1 + \frac{4\langle H_I \rangle^2/\hbar^2}{(2\omega - \omega_{P_{1/2}} - \omega_{P_{3/2}} - \frac{C^{(3)}_{1/2}}{R^3} - \frac{C^{(3)}_{3/2}}{R^3})^2 + \Gamma^2} + \frac{4(2\omega - \omega_{P_{1/2}} - \omega_{P_{3/2}} - \frac{C^{(3)}_{1/2}}{R^3} - \frac{C^{(3)}_{3/2}}{R^3})\langle H_I \rangle/\hbar}{(2\omega - \omega_{P_{1/2}} - \omega_{P_{3/2}} - \frac{C^{(3)}_{1/2}}{R^3} - \frac{C^{(3)}_{3/2}}{R^3})^2 + \Gamma^2} \Bigg]. \quad (2)$$

This model, presented in Eq. (2), has a good agreement with the behavior of the asymmetric part of the peak, demonstrating that asymmetry comes from the potential dependence on R, and not from hyperfine states, unlike the asymmetry present in the peaks centered at $\omega_{P_{1/2}}$ and $\omega_{P_{3/2}}$.

Although we have good agreement on the red side of the peak, we do not have the same for the maximum of the peak. The constructed model [Eq. (2)] predicts a much faster increase around the peak (factor of 4), and the frequency where the maximum is obtained appears to be displaced further to the blue in the model. In reality, as excitation approaches the peak, we are also approaching both the hyperfine splitting of the ground state (1.7 GHz) and the hyperfine state manifold for the excited states (0.2 GHz). In this region, the combination of the molecular levels produces a complex "spaghetti" of levels [12] already explored in cold atomic collisions. This complex level structure invalidates the simplified level structure considered in the model. To construct a more realistic model, such facts must be taken into account, but such a construction is far beyond the scope of this Letter.

Finally, we should point out that the two-photon cooperative absorption in cold atoms may open up a new, exciting nonlinear type of effect which may allow investigation into the process of cold-atom interactions in classical or quantum degenerate samples. The process is by itself a way to generate entanglement [13] of atoms in the excited state as well as to produce correlated photons with different frequencies [14,15]. Both of those effects may find interesting applications in the future.

We have demonstrated the occurrence of two-photon cooperative absorption in a sample of cold Na atoms. The topic of nonlinearities in colliding cold atoms has potential for many applications, and this first demonstration may stimulate further investigations.

The authors thank Daniel Magalhães, Marcelo Martinelli, and Miled Moussa for fruitful discussions and suggestions, and FAPESP (CEPID), CNPq (INCT), and CAPES for the financial support.

[1] J. Weiner, V. S. Bagnato, S. Zilio, and P. S. Julienne, Rev. Mod. Phys. **71**, 1 (1999).
[2] J. C. White, Opt. Lett. **6**, 242 (1981).
[3] J. R. Rios Leite and C. B. De Araujo, Chem. Phys. Lett. **73**, 71 (1980).
[4] D. L. Andrews and M. J. Harlow, J. Chem. Phys. **78**, 1088 (1983).
[5] J. W. R. Tabosa, S. S. Vianna, and F. A. M. de Oliveira, Phys. Rev. A. **55**, 2968 (1997).
[6] E. L. Raab, M. Prentiss, A. Cable, S. Chu, and D. E. Pritchard, Phys. Rev. Lett. **59**, 2631 (1987).
[7] R. R. de Paiva, R. Muhammad, R. F. Shiozaki, A. L. de Oliveira, D. V. Magalhães, J. Ramirez-Serrano, V. S. Bagnato, and K. M. F. Magalhães, Laser Phys. Lett. **6**, 163 (2009).
[8] D. S. Durfee, Ph.D. thesis, MIT, 1999.
[9] D. M. B. P. Milori, A. M. Tuboy, L. G. Marcassa, R. Habesch, S. C. Zilio, and V. S. Bagnato, Laser Phys. **8**, 1163 (1998).
[10] V. Bagnato, L. Marcassa, C. Tsao, Y. Wang, and J. Weiner, Phys. Rev. Lett. **70**, 3225 (1993).
[11] A. Gallagher, Phys. Rev. A **44**, 4249 (1991).
[12] P. D. Lett, P. S. Julienne, and W. D. Phillips, Annu. Rev. Phys. Chem. **46**, 423 (1995).
[13] A. Einstein, B. Podolsky, and N. Rosen, Phys. Rev. **47**, 777 (1935).
[14] M. D. Reid, P. D. Drummond, W. P. Bowen, E. G. Cavalcanti, P. K. Lam, H. A. Bachor, U. L. Andersen, and G. Leuchs, Rev. Mod. Phys. **81**, 1727 (2009).
[15] M. D. Lukin, Rev. Mod. Phys. **75**, 457 (2003).